

# The First Light Curve Solutions and Period Study of BQ Ari

Atila Poro<sup>1</sup>, Fatemeh Davoudi<sup>1</sup>, Fahri Alicavus<sup>2,3</sup>, Ekrem Murat Esmer<sup>4</sup>, Ozgur Basturk<sup>4</sup>, Nazim Aksaker<sup>5,6</sup>, Somayah Khakpash<sup>7</sup>, Aysun Akyüz<sup>6,8</sup>, Yasemin Aladağ<sup>6</sup>, Jabar Rahimi<sup>1</sup>, Elahe Lashgari<sup>1</sup>, Amin Boudesh<sup>1</sup>, Morteza Ghanbarzadehchaleshtori<sup>1</sup>, Sima Modarres<sup>1</sup>, Ali Sojoudizadeh<sup>1</sup>, Arif Solmaz<sup>6</sup>, Mahmut Tekeş<sup>6</sup>

<sup>1</sup>The International Occultation Timing Association Middle East section, Iran, info@iota-me.com

<sup>2</sup>Çanakkale Onsekiz Mart University, Faculty of Arts and Sciences, Department of Physics, 17020, Çanakkale, Turkey

<sup>3</sup>Çanakkale Onsekiz Mart University, Astrophysics Research Center and Ulupinar Observatory, 17020, Çanakkale, Turkey

<sup>4</sup>Ankara University, Faculty of Science, Astronomy and Space Sciences Department, TR-06100, Tandogan, Ankara, Turkey

<sup>5</sup>Adana Organised Industrial Zones Vocational School of Technical Science, University of Çukurova, 01410, Adana, Turkey

<sup>6</sup>Space Science and Solar Energy Research and Application Center (UZAYMER), University of Çukurova, 01330, Adana, Turkey

<sup>7</sup>Department of Physics and Astronomy, University of Delaware, Newark, DE 19716, USA

<sup>8</sup>Department of Physics, University of Çukurova, 01330, Adana, Turkey

## Abstract

The first complete analysis of the photometric observation of the W UMa type binary system BQ Ari was performed using the Wilson-Devinney (W-D) code combined with a Monte Carlo (MC) simulation to determine its photometric and geometric elements, and their uncertainties. These results show that BQ Ari is a contact binary system with a photometric mass ratio  $q = 0.548 \pm 0.018$ , a fillout factor  $f = 24\%$ , and an orbital inclination of  $i = 85.09 \pm 0.45$ . We calculated the distance of BQ Ari to be  $128 \pm 19$  parsecs from the combined brightness of the system, which is in agreement with the distance value derived from the Gaia parallax ( $132.848 \pm 1.574$ ) in one standard deviation of the calculated value. In this study, we suggested a new linear ephemeris for BQ Ari, combining our new mid-eclipse times and the previous observations, which we analyzed using Monte Carlo Markov Chain (MCMC) method. We present the first analysis of the system's orbital period behavior and analysis of the O-C diagram using the Genetic Algorithm (GA) and the MCMC approaches in OCFit code. We attempted to explain the analysis of the residuals of linear fit in the O-C diagram with two approaches; "LiTE + Quadratic" and "Magnetic activity + Quadratic". Although we consider the magnetic activity to be probable, the system should be followed up to reveal the nature of orbital period variations in it. Additional observations will be needed to reveal the reasons behind the observed-period changes in this binary system. Hence these models can be considered as suggestions for future reference.

## Keywords

Techniques: photometric; Stars: binaries: eclipsing; Stars: individual: BQ Ari

## 1 Introduction

BQ Ari is a W UMa type eclipsing binary star in the constellation of Aries. W UMa eclipsing variables are the most abundant types of close binary stars (Shapley 1948). In such systems, both stars have a common connective envelope (Lucy 1967) and their components fill their Roche lobes (Kopal 1959). These contact binaries are detached systems in the early stages of their evolution and they may go through different physical phenomena throughout their lifetimes. Astronomers analyze these observed phenomena to understand why and how the components come in contact with each other. One potential explanation, is the Angular Momentum Loss (AML) via magnetic braking by stellar winds (Eggen & Iben 1989) which can lead to the contact phase (Stępień 2006). On the other hand, Qian (2018) asserted that a detached system evolves into a contact binary in a relatively short period of time when a large fraction of angular momentum is transferred to a third body. Therefore, there is a probability that the mass ratio is reversed. In order to address this issue, it is important to investigate the contact binaries in which the mass ratio is close to unity (Li 2020). W UMa contact binaries are considered as one of the good tools for distance determinations. In addition, the radii of individual components are measured through period studies. Absolute magnitude is also obtained via the radius estimation along with the color information. Hence, the distances of the eclipsing binaries can be determined from the luminosity and observed fluxes (Rucinski 1996). These distances are used as calibration sources to verify distances derived by other

methods. Furthermore, studies of orbital variations observed in close binaries provide us with invaluable details about the mass transfer or mass loss of these systems. According to a study based on the data of 159 close binary systems by Csizmadia & Klagyivik (2004), mass and luminosity ratio play important role in estimating the rate of energy transfer between components.

The variability of BQ Ari (GSC 00646-00946) was first discovered in the All-Sky Automated Survey (ASAS<sup>1</sup>) project and classified as a contact binary system. BQ Ari's apparent magnitude in *V* filter is 11.97 (APASS9<sup>2</sup>), and it has an orbital period of 0.282333 days (Paschke 2011).

In this paper, we aim to find the Roche configuration and evolutionary state of BQ Ari through its photometric analysis. It is worth mentioning that we have made use of Python codes written by us for increasing the accuracy to compute the mid-eclipse times from our own observations and their timing uncertainties, as well as presenting a new ephemeris based on Monte Carlo Markov Chain (MCMC) method. We then analyze the observed orbital period variations of the system using MCMC approaches. Furthermore, we performed the first light curve analysis to determine the absolute parameters of BQ Ari, and its uncertainties with the Monte Carlo (MC) simulation. This paper and other similar studies help to conduct comparative studies to figure out more about the formation and evolution stages of contact binaries.

## 2 Observation and data reduction

The photometric observations of BQ Ari were carried out with a 50 cm Ritchey Chretien telescope and Apogee Aspen CG type CCD during four nights of observation at the UZAYMER Observatory, Çukurova University, Adana, Turkey on the 7<sup>th</sup> and 15<sup>th</sup> of December 2019 and the 13<sup>th</sup> and 15<sup>th</sup> of January 2020. The CCD attached on the telescope has a 1024×1024 pixel array with a pixel length of 24 $\mu$ . In these observations we used the *BVR* standard Johnson filters. Each of the frames was 1×1 binned with 40s exposure time for *R* filter, 60s for *V* filter, and 85s for the *B* filter; the average temperature of the CCD was -45°C during four nights of observations. A total of 1281 images were acquired in the *BVR* filters. Observations through *V* and *R* filters were performed for each filter in one single night and in the *B* filter during two other nights.

GSC 646-868 and TYC 646-333-1 were chosen as comparison stars, and GSC 646-726 was selected as the reference star. All of these stars are close to BQ Ari and the magnitude of the reference star is appropriate for precise differential photometry. The characteristics of the comparisons and reference stars are shown in Table 1.

**Table 1.** Characteristics of the variable, comparison and reference stars (from: Vizier-APASS9).

Type	Star	Magnitude ( <i>V</i> )	RA. (J 2000)	Dec. (J 2000)
Variable	BQ Ari	11.97	02 48 41.07	+13 45 06.65
Comparison <sub>1</sub>	GSC 646-868	12.77	02 48 36.48	+13 43 28.69
Comparison <sub>2</sub>	TYC 646-333-1	10.93	02 48 27.00	+13 44 58.73
Reference	GSC 646-726	12.56	02 48 34.14	+13 43 53.17

We reduced the raw images and corrected them. The basic data reduction was performed for bias, dark and flat field of each CCD image according to the standard method. We aligned, reduced, and plotted raw images with the AstrolmageJ (AIJ) software (Collins et al. 2017). AIJ provides an astronomy-specific image display environment and tools for astronomy-specific image calibration and data reduction. This software can be also used to determine the best linear fit to a dataset (See for example Davoudi et al. 2020).

## 3 Light curve analysis

We analyzed our light curves using the Wilson & Devinney (1971) code (W-D). The well-known *q*-search method was first run to have an estimate of the mass ratio of the binary system. The *q*-search analysis gives reliable mass

<sup>1</sup><http://www.astrouw.edu.pl/asas/>

<sup>2</sup><http://vizier.u-strasbg.fr/>

ratios when full-eclipses are observed in the light curve (Kjurkchieva 2019). We found the minimum sum of the squared residuals of the W-D fit,  $\sum(O - C)^2$ . As a result, a range of fixed mass ratios from 0.1 to 5 was used to search as shown in Figure 1. When the  $q$ -search results are examined, it is seen that it has almost the same sum of residuals values, especially in the range of 0.5-1.1. This is particularly common in contact binary stars. We use the W-D code combined with the MC simulation to reduce degeneration in the solution space and determine the uncertainties of the adjustable parameters (Zola et al. 2004, 2010). The free parameters in MC and their ranges are given in the Table 2.

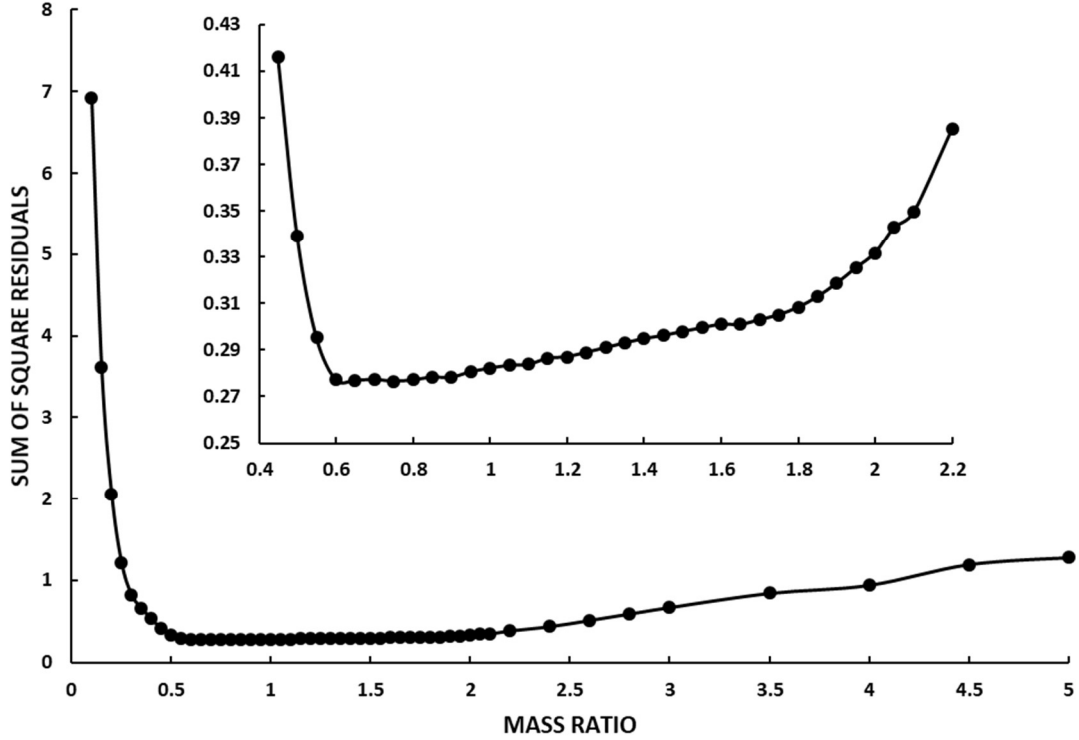


Fig 1. Sum of the squared residuals as a function of the mass ratio.

Table 2. Free parameters and search ranges in MC Simulations.

Parameter	Value
$i$ (deg)	60-90
$T_2$ (K)	5000-5700
$\Omega_{1,2}$	1.9-10
$q = (m_2/m_1)$	0.1-6
$l_1$	4-12.0
Phase shift	-0.03-0.03
co-latitude (deg)	0-180
Longitude (deg)	0-360
Spot radius (deg)	1-90
$T_{\text{spot}}/T_1$	0.7-1

Based on our data and after the required calibrations (Høg et al. 2000), we calculated  $(B - V)_{BQ\ Ari} = 0^m.65$ . Thus, the effective temperature of the primary component,  $T_1$  was assumed as 5559 K (Eker et al. 2020). This temperature value is a good approximation because we can compare it with that from the Gaia DR2<sup>3</sup> catalog which is  $5498^{+251}_{-166}$  K; Based on the Gaia color BP-RP, the difference in temperature is consistent. We fixed some

<sup>3</sup><https://www.cosmos.esa.int/web/gaia/dr2>

parameters and assumed gravity-darkening coefficients of  $g_1 = g_2 = 0.32$  (Lucy 1967) and bolometric albedos of  $A_1 = A_2 = 0.5$  (Rucinski 1969) for stars with convective envelopes and linear limb darkening coefficients were taken from the tables published by Van Hamme (1993). The parameters and their errors obtained from the light curve analysis in the *BVR* filters are presented in Table 3 and the synthetic light curves based on these parameters are given in Figure 2 together with the residuals from the models.

**Table 3.** Photometric solutions of BQ Ari.

Parameter	Results
$T_1$ (K)	5498(200)
$T_2$ (K)	5497(209)
$\Omega_1=\Omega_2$	2.8877(299)
$i$ (deg)	85.09(45)
$q$	0.548(18)
$l_1/l_{tot}(B)$	0.622(6)
$l_2/l_{tot}(B)$	0.378(4)
$l_1/l_{tot}(V)$	0.622(6)
$l_2/l_{tot}(V)$	0.378(4)
$l_1/l_{tot}(R)$	0.622(6)
$l_2/l_{tot}(R)$	0.378(4)
$A_1=A_2$	0.50
$g_1=g_2$	0.32
$f$ (%)	24(8)
$r_1$ (back)	0.4821(50)
$r_1$ (side)	0.4479(46)
$r_1$ (pole)	0.4197(43)
$r_2$ (back)	0.3787(39)
$r_2$ (side)	0.3369(35)
$r_2$ (pole)	0.3205(33)
$r_1$ (mean)	0.449(5)
$r_2$ (mean)	0.345(4)
Colatitude <sub>spot</sub> (deg)	20.5(1.3)
Longitude <sub>spot</sub> (deg)	59.8(2)
Radius <sub>spot</sub> (deg)	48.8(1.7)
$T_{spot}/T_{star}$	0.83(2)
Phase Shift	0.0208(2)

Notes: Parameters of a star spot on the primary component.

The fillout factor was calculated as 24% from the output parameters of the light curve solutions via,

$$f = \frac{\Omega(L_1) - \Omega}{\Omega(L_1) - \Omega(L_2)} \quad (1)$$

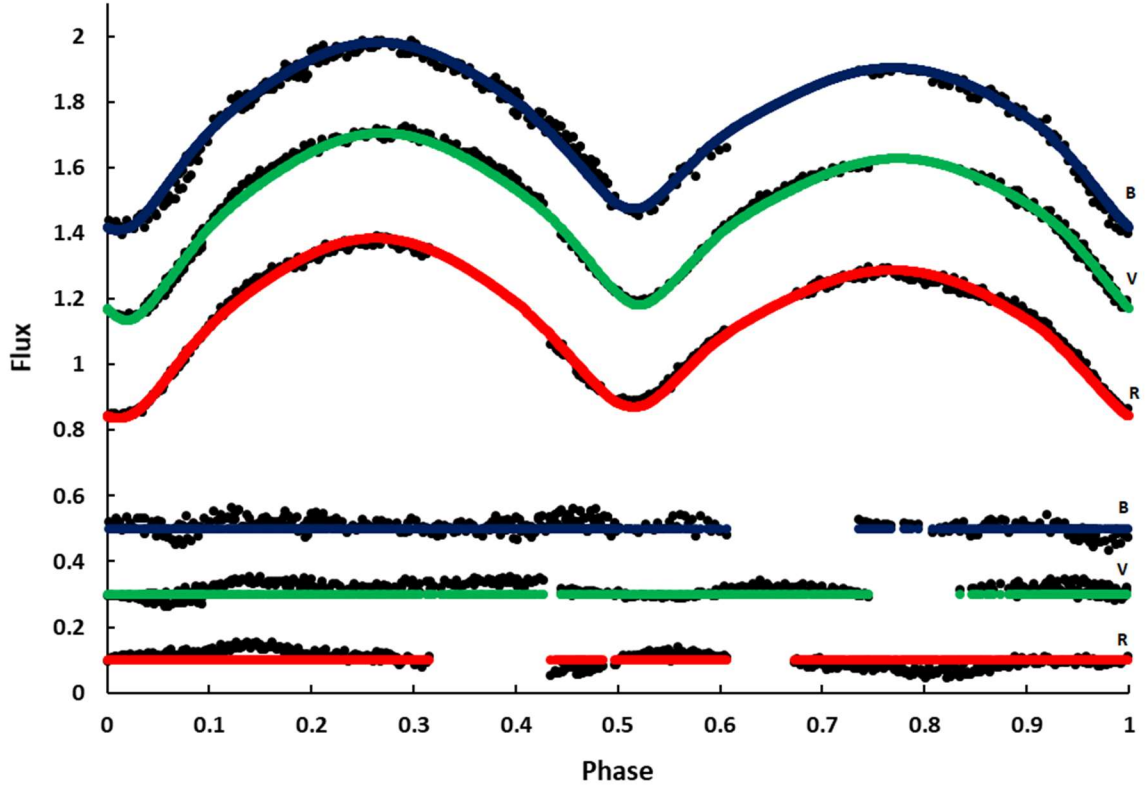


**Fig 2.** The observed light curves of BQ Ari (black dots), and synthetic light curves obtained from light curve solutions in the B, V, and R filters (top to bottom respectively) and residuals are plotted; with respect to orbital phase, shifted arbitrarily in the relative flux.

The absolute parameters of BQ Ari are calculated and given in Table 4. The mass of the primary component is derived from a study by Eker et al. (2020), and the mass of the secondary component is calculated based on the value of  $q$ . Since the radial velocity is not yet available, we were unable to determine the masses of the components with high precision through photometry; we are only able to make reliable estimates here.

**Table 4.** Estimated absolute elements of BQ Ari.

Parameter	Primary	Secondary
$Mass (M_{\odot})$	0.979(40)	0.536(28)
$Radius (R_{\odot})$	0.933(16)	0.717(15)
$Luminosity (L_{\odot})$	0.713(11)	0.421(6)
$M_{bol}$ (mag)	5.11(36)	5.68(41)
$\log g$ (cgs)	4.489(23)	4.456(30)
$a (R_{\odot})$	2.079(22)	

The mean fractional radii of components are 0.449 and 0.345 for the primary and secondary components, respectively; these values were calculated from the formula,  $r_{mean} = (r_{pole} \times r_{side} \times r_{back})^{\frac{1}{3}}$ . Also, the radii of the components were computed using the formula  $R = a \times r_{mean}$  as 0.933 ( $R_{\odot}$ ) and 0.717 ( $R_{\odot}$ ) for the primary and secondary, respectively. As a result, the binary system is in a marginal contact state (Kopal 1959) since the sum of the mean fractional radii of the components is  $r_{mean} = r_{1mean} + r_{2mea} = (0.79) > 0.75$ .

One of the interesting characteristics of W Uma binaries is the well-known O'Connell effect (O'Connell 1951) that is described by the asymmetry in the brightness of maxima in the light curve of eclipsing binary star systems. The most appropriate suggestion for this effect is the presence of star spot(s) induced by the magnetic activities of the components (Sriram et al. 2017).

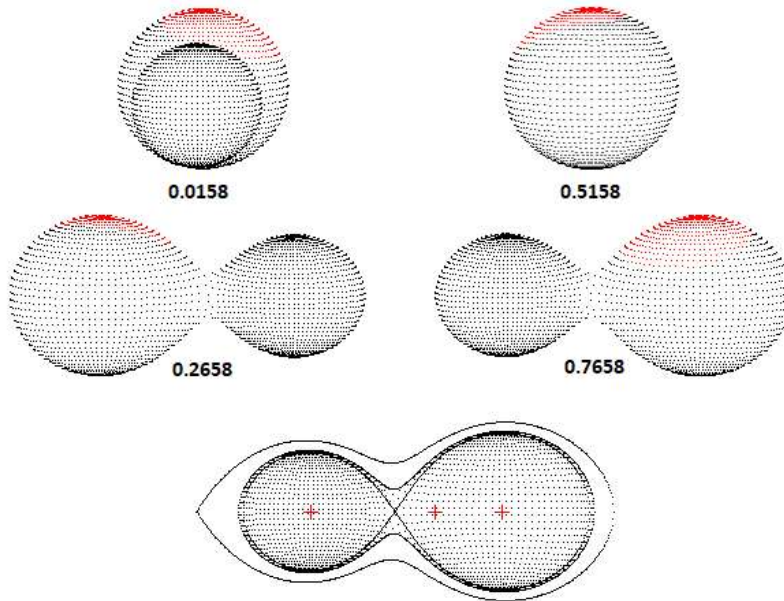
The light curves of BQ Ari in the  $B$ ,  $V$ , and  $R$  bands (Figure 2) indicate the presence of the O'Connell effect in this system, whereby  $Max I$  is brighter than  $Max II$  ( $Max I > Max II$ ) and asymmetry in maxima or unequal minima is visible clearly. Due to the presence of asymmetry in light curves, we used a stellar spot during the light curve solution in all three  $BVR$  filters and cool spot on the massive primary component results in an acceptable solution for all  $BVR$  light curves (Table 3).

Table 5 represents BQ Ari's characteristic parameters of its light curves and it also shows the difference in maxima with each filter in the first row. Accordingly, the largest difference between the levels of maximum light and the depths of the minima were observed in the  $B$  filter; while they were the smallest in the  $R$  filter, which is expected from the magnetic activity-induced variations.

**Table 5.** Characteristic parameters of the light curves in  $BVR$  filters.

Light curve	$\Delta B$	$\Delta V$	$\Delta R$
$MaxI - MaxII$	-0.097	-0.088	-0.082
$MaxI - MinII$	-0.794	-0.801	-0.552
$MaxI - MinI$	-0.956	-0.909	-0.600
$MinI - MinII$	0.162	0.108	0.048

The positions of the components are shown in Figure 3 for four different orbital phases during an orbital period. The cold spot is on the primary star.



**Fig 3.** The positions of the components of BQ Ari.

The total eclipse corresponding to the secondary minima enabled us to compute the visual magnitude of the primary component as  $V_{pri.} = 10^m.876 \pm 0.004$ . We found the spectral type of components as G8 for the primary and secondary, and the bolometric correction ( $BC$ ) =  $-0.063$  from Eker et al. (2020) with using  $T_1$  which is coming from Gaia DR2. We have presented the  $M_{bol}$  in Table 4; the calculated absolute magnitude of components is defined by Equation (2).

$$M_V = M_{bol} - BC_V \quad (2)$$

Therefore, value of  $M_v = 5^m.17 \pm 0.02$  was obtained for the primary component. To calculate the distance of a star, we must consider the scattering and absorption of light due to the passage of light through the dust grains in the InterStellar Medium (ISM). Due to this phenomenon, the star appears to be dimmer and redder. In order

to account for this effect, the extinction,  $A_V$ , should be estimated.  $A_V$  is related to the interstellar reddening,  $E(B - V)$ , by the Equation (3) where  $R_V$  is a normalizing coefficient.

$$A_V = (R_V) \times E(B - V) \quad (3)$$

$E(B - V)$  is obtained using a method introduced by Schlafly & Finkbeiner (2011), which is based on Fitzpatrick (1999) reddening law and the results of the Schlegel et al. (1998) dust maps with a calibration coefficient of 0.86. According to that, the value of  $E(B - V)$  is found to be  $0.1127 \pm 0.0068$ . Considering the coefficient  $R_V = 3.1$ , the extinction was calculated to be  $A_V = 0.349 \pm 0.021$  and  $A_{dV} = 0.175 \pm 0.021$ . Based on these calculations, the distance ( $d$ ) to the binary system was estimated to be  $d_{(pc)} = 128 \pm 19$  using Equation (4).

$$d_{(pc)} = 10^{\left(\frac{V_{pri} - A_V - M_{pri} + 5}{5}\right)} \quad (4)$$

The Gaia parallax, which is corrected for the systematic shift of 0.082 mas as given by Stassun & Torres (2018), gives a distance value of  $132.848 \pm 1.574$  pc. Our estimated distance found from the combined bolometric magnitude of the system seems to be consistent with the Gaia distance considering our estimated uncertainty.

#### 4 Determination of Mid-Eclipse Times

Before analyzing period changes, it is necessary to find the times of minima in the light curves. This is commonly achieved using the Kwee and van Woerden (1956) method (KW method) by compute the mid-eclipse times from the binary system's light curves. Despite it is a well-established method to derive times of minima, the KW method underestimates the uncertainties and the estimated errors are usually unrealistically small (Li et al. 2018; Pribulla et al. 2012). Furthermore, it may not be adequate in the case of asymmetric data or an incomplete light curve due to its nature (Mikulášek et al. 2013). To find the times of the minima, we fit models based on Gaussian and Cauchy distributions to selected portions of the light curves that include the minima. We then used the MCMC sampling methods to estimate the uncertainty of the values. The code is implemented in Python using the PyMC3 package (Salvatier et al. 2016).

#### 5 Orbital Period Variations

A trend in the orbital period variations, indicated by the deviations of observed mid-eclipse times (O) from their calculated values (C) based on a reliable ephemeris, so called the O-C variations, is generally a combination of different effects. Formally, it is written as

$$\delta T_i = (\Delta T_0 + \Delta P \times E) + Q \times E^2 + \delta T_i \quad (5)$$

where the part in parentheses generates a linear trend in (O-C)s and it is caused by a linear ephemeris. The quadratic term describes changes due to mass transfer. The term  $\delta T_i$  implies more complex periodic variations in (O-C)s (Gajdoš and Parimucha 2019).

We collected 22 mid-eclipse times from the literature and obtained 8 individual mid-eclipse times from our observations which are shown in Table 6. Mid-eclipse times identified as Min (BJD<sub>TDB</sub>), are in column 1; their uncertainties appear in column 2 (some of the observers didn't provide their uncertainties and we assumed the mean error value for these data points). Minima types (I: primary and II: secondary) are in column 3; epochs of these minima times are in column 4; O-C values are in column 5; and the references of mid-eclipse times are shown in the last column. The epochs and the O-C values were calculated by the following linear ephemeris (Školník 2017),

$$Min. I (BJD_{TDB}) = 2458043.4658 + 0.282335 \times E. \quad (6)$$

**Table 6.** Times of minima of BQ Ari obtained by CCD.

Min (BJD <sub>TDB</sub> )	Error	Min Type	Epoch	O-C	Reference
2454800.2868	0.0007	I	-11487	0.0031	Hubscher 2010
2455593.3617	0.0020	I	-8678	-0.0010	Paschke 2011
2455866.3787		I	-7711	-0.0019	Hübscher et al. 2012
2456563.4603	0.0009	I	-5242	-0.0054	Hübscher 2014
2456563.6023	0.0010	II	-5241.5	-0.0046	Hübscher 2014
2456573.4835	0.0004	II	-5206.5	-0.0051	Zasche et al. 2014
2456573.6258	0.0002	I	-5206	-0.0040	Zasche et al. 2014
2456908.8967	0.0002	II	-4018.5	-0.0059	AAVSO <sup>4</sup>
2456932.4762	0.0005	I	-3935	-0.0014	Zasche et al. 2017
2456959.4340	0.0005	II	-3839.5	-0.0066	Zasche et al. 2017
2457277.4881	0.0006	I	-2713	-0.0029	Zasche et al. 2017
2457320.2625		II	-2561.5	-0.0022	Nagai 2016
2457331.4158	0.0030	I	-2522	-0.0011	Paschke 2017
2457331.5568	0.0040	II	-2521.5	-0.0013	Paschke 2017
2457385.3411	0.0017	I	-2331	-0.0018	Hübscher 2017
2457385.4831	0.0024	II	-2330.5	-0.0010	Hübscher 2017
2457657.5134	0.0001	I	-1367	-0.0005	Pagel 2018
2457728.2391	0.0002	II	-1116.5	0.0003	Ozavci et al. 2019
2458043.4658	0.0006	I	0.0	0.0000	Školník 2017
2458043.6081	0.0009	II	0.5	0.0011	Školník 2017
2458438.3107	0.0041	II	1398.5	-0.0006	Pagel 2019
2458438.4518	0.0026	I	1399	-0.0007	Pagel 2019
2458825.24922	0.00005	I	2769	-0.0022	This study
2458825.39096	0.00007	II	2769.5	-0.0016	This study
2458833.15474	0.00009	I	2797	-0.0021	This study
2458833.29519	0.00011	II	2797.5	-0.0028	This study
2458833.43720	0.00010	I	2798	-0.0019	This study
2458862.23527	0.00017	I	2900	-0.0020	This study
2458864.21285	0.00016	I	2907	-0.0008	This study
2458864.35428	0.00027	II	2907.5	-0.0005	This study

We computed the O-C values based on the reference minimum and the orbital period in Equation 6 and fitted all mid-eclipse times with a line using a code that we wrote based on the emcee package in Python as shown in Figure 4. We used a least-squares approach to have a first estimate on  $\Delta P$  and  $\Delta T_0$  as initial values to MCMC and using MCMC determine new linear ephemeris for the primary minimum. In MCMC we made use of 200 random walkers in 10000 steps the first 100 of each walker were ignored (burn-in = 100) to fix the chains at a certain value for slope and y-intercept of the line; the slope being the change of the period and y-intercept is the change in the reference mid-eclipse time; As a result, we have obtained the posterior probabilities for these parameters (Figure 5). Consequently, we refined the ephemeris based on the combination of our own mid-eclipse times and those from previous observations, as

$$Min. I (BJD_{TDB}) = (2458043.4673043_{-0.0005635}^{+0.0004675}) + (0.28233566_{-0.00000024}^{+0.00000019}) \times E \text{ days} \quad (7)$$

where  $E$  is the integer number of orbital cycles after the reference epoch.

<sup>4</sup><https://www.aavso.org/>



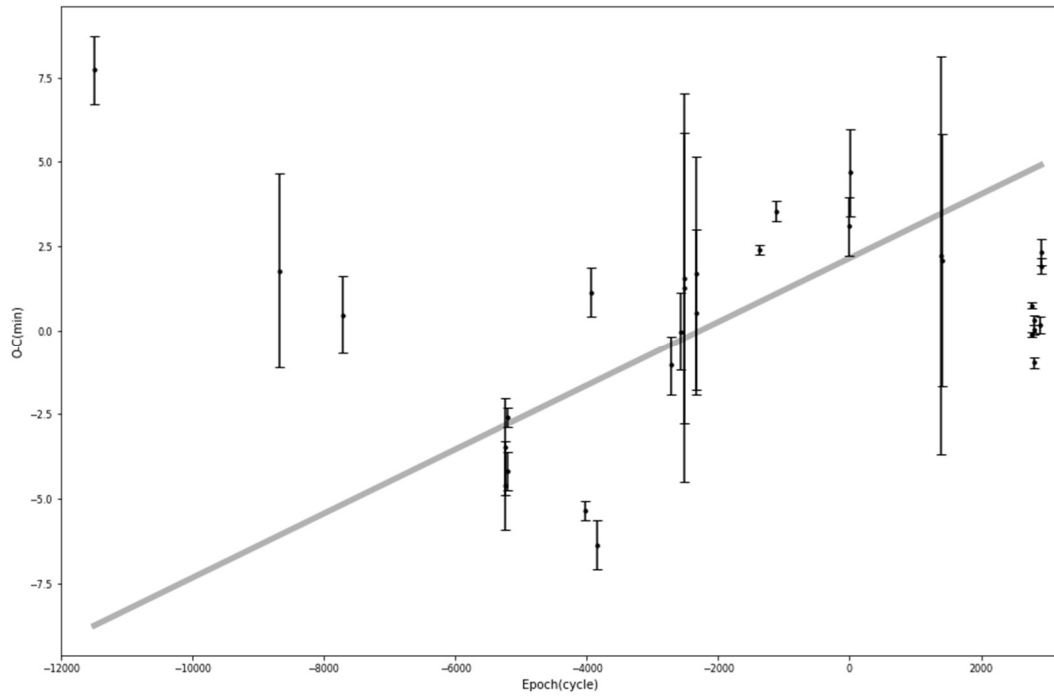


**Fig 4.** The initial O-C diagram of BQ Ari with the linear trend on the data using the MCMC method.

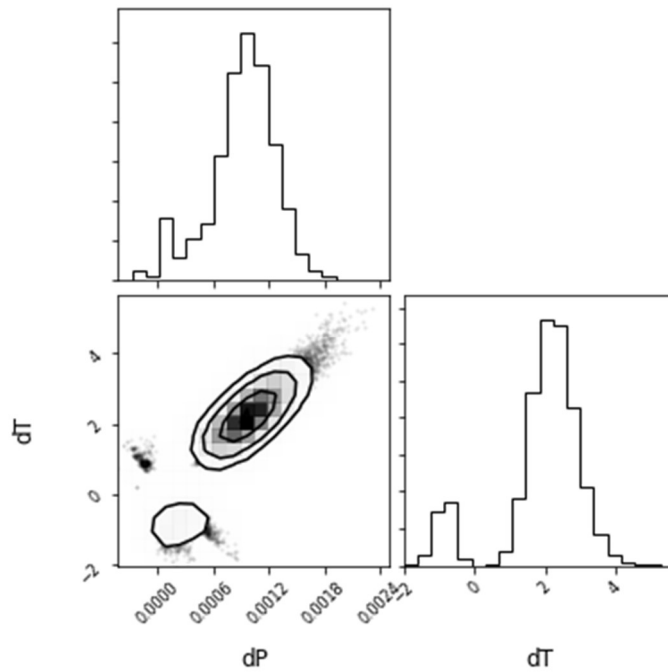


**Fig 5.** Corner plot showing the two-dimensional probability distributions of  $dT$  and  $dP$  and the histograms posterior probability distribution of both.

After subtracting the linear trend from the original O-C, the residue (O-C) diagram (the residue between original values of this O-C and O-C's calculated from the fit), is plotted in Figure 6 concerning new linear ephemeris (Equation 7).

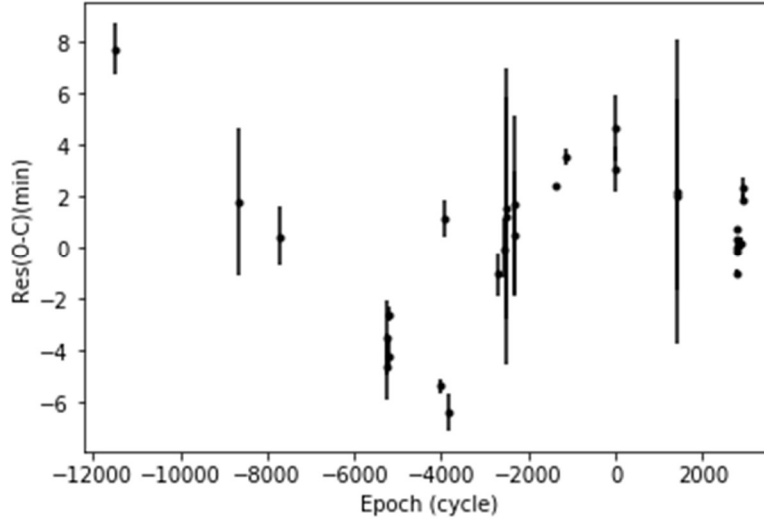


Fig 6. The residue O-C diagram of BQ Ari.

We have used a Lomb-Scargle Periodogram to search for a periodicity in the frequency space (Figure 7). False alarm probabilities of 0.1%, 1%, and 5% (FAPs) are displayed on the Periodogram as an indication of courier reliability.

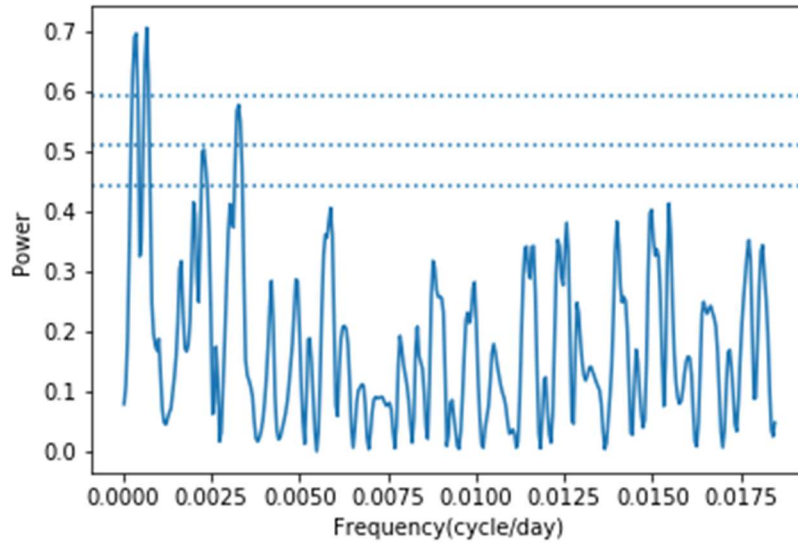


Fig 7. Lomb-Scargle Periodogram of residuals O-C. FAPs = 0.1%, 1% and 5% from up to down are indicated with dotted horizontal lines.

The cyclic trend in the residuals of O-C diagram in this system can be caused either by Light-Time Effect (LiTE) due to the existence of a third body or the magnetic activity cycles of the system (Pi, Q.F., Zhang et al. 2017). We investigated each of these cases to explain the variations in the residuals. At first, we checked the LiTE next to the quadratic trend, (the (O-C) diagram in Figure 8) and obtained the parameters of LiTE induced by the presence of a potential third companion in the system (Table 7). They were derived with the GA and the MCMC approach using the OCFit code. The GA removes the necessity of any input values of the model's parameters. Final values of them together with their statistically significant uncertainties were obtained using MCMC fitting. The combination of these two algorithms allowed us to analyze the exact physical model of the observed variations. The number of generations and the size of one generation were both regarded as 2500 as parameters of GA. Also, we employed 100000 iterations and burn-in=5000 for the O-C diagram in our MCMC runs. Confidence

interval graphs for fitted parameters and histograms of various parameters were determined by the MCMC simulation displayed in Figure 9 and Figure 10, respectively.

The sinusoidal term suggests a periodic change with a period of 8.10 years and an amplitude of 4.455 minutes. The analytical formula for O-C changes caused by LiTE, where the semi-amplitude of changes on the O-C diagram generated by LiTE is given by the equation (Irwin 1952),

$$K_3 = \frac{a_{12} \sin i_3 \sqrt{1 - e_3^2} \cos \omega_3}{c} \quad (8)$$

where  $a_{12} \sin i_3$  is the projected semi-major axis of the binary star around the barycenter of a triple system,  $i_3$  is the inclination of the third body's orbit,  $e_3$  is the eccentricity and  $\omega_3$  is the argument of periastron. Computation with the following equation yields a large mass function of  $f(m_3) = 0.003 M_\odot$  for the third companion (Irwin 1952),

$$f(m_3) = \frac{(a_{12} \sin i_3)^3}{p_3^2} \quad (9)$$

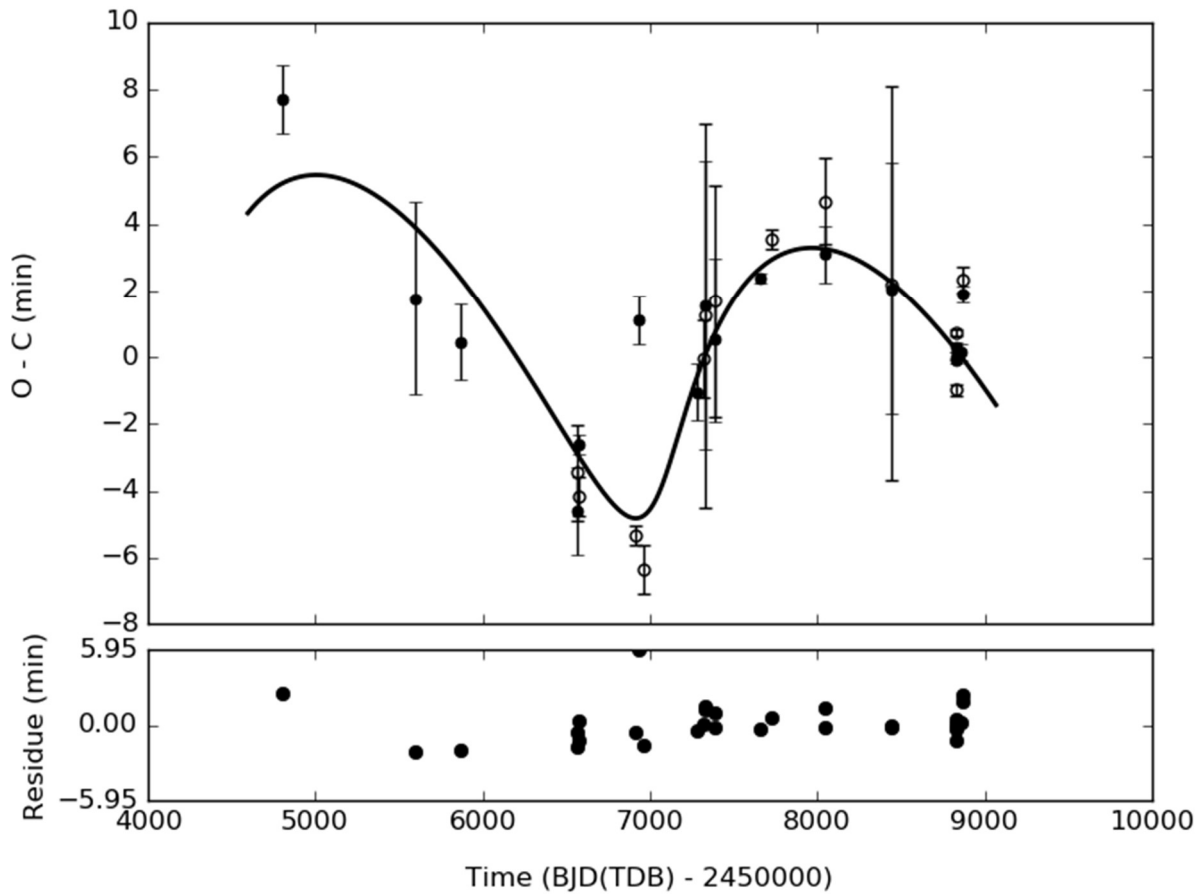


**Fig 8.** The O-C diagram of BQ Ari with the periodic trend on the data points induced by the LiTE + Quadratic effect.

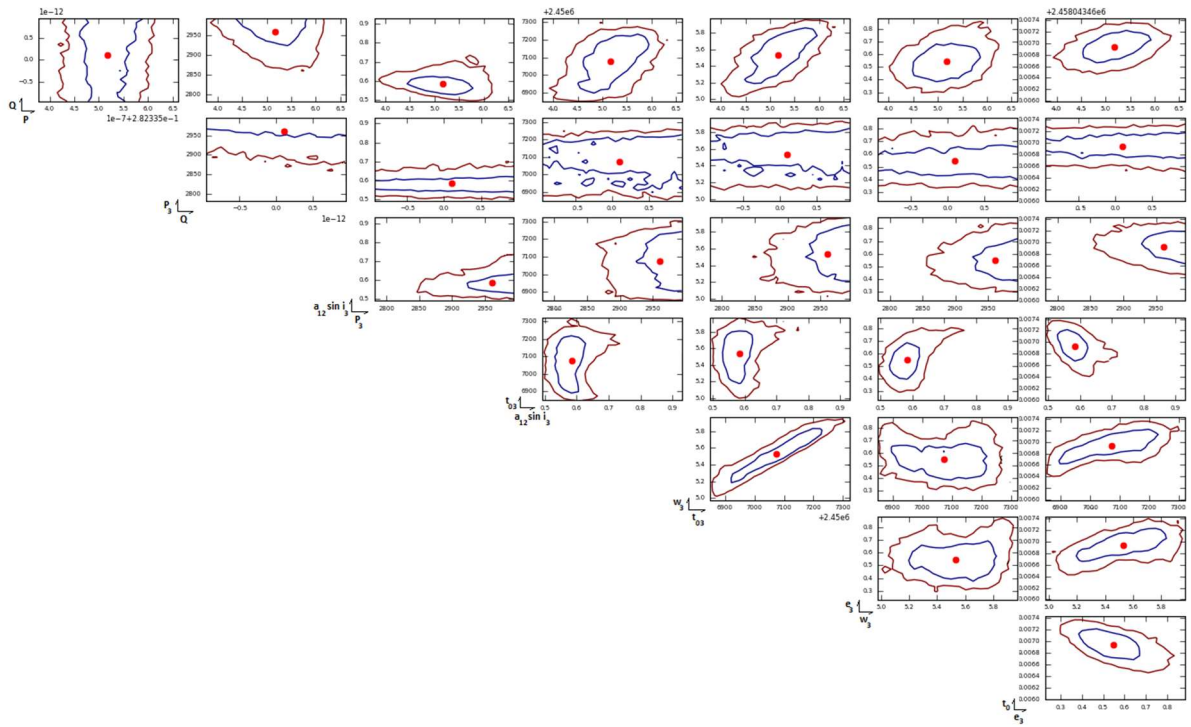


**Fig 9.** Confidence interval graphs for fitted parameters determined by the MCMC simulation for the LiTE + Quadratic model. A red dot shows a solution and the three irregular regions display  $1\sigma$ ,  $2\sigma$ .

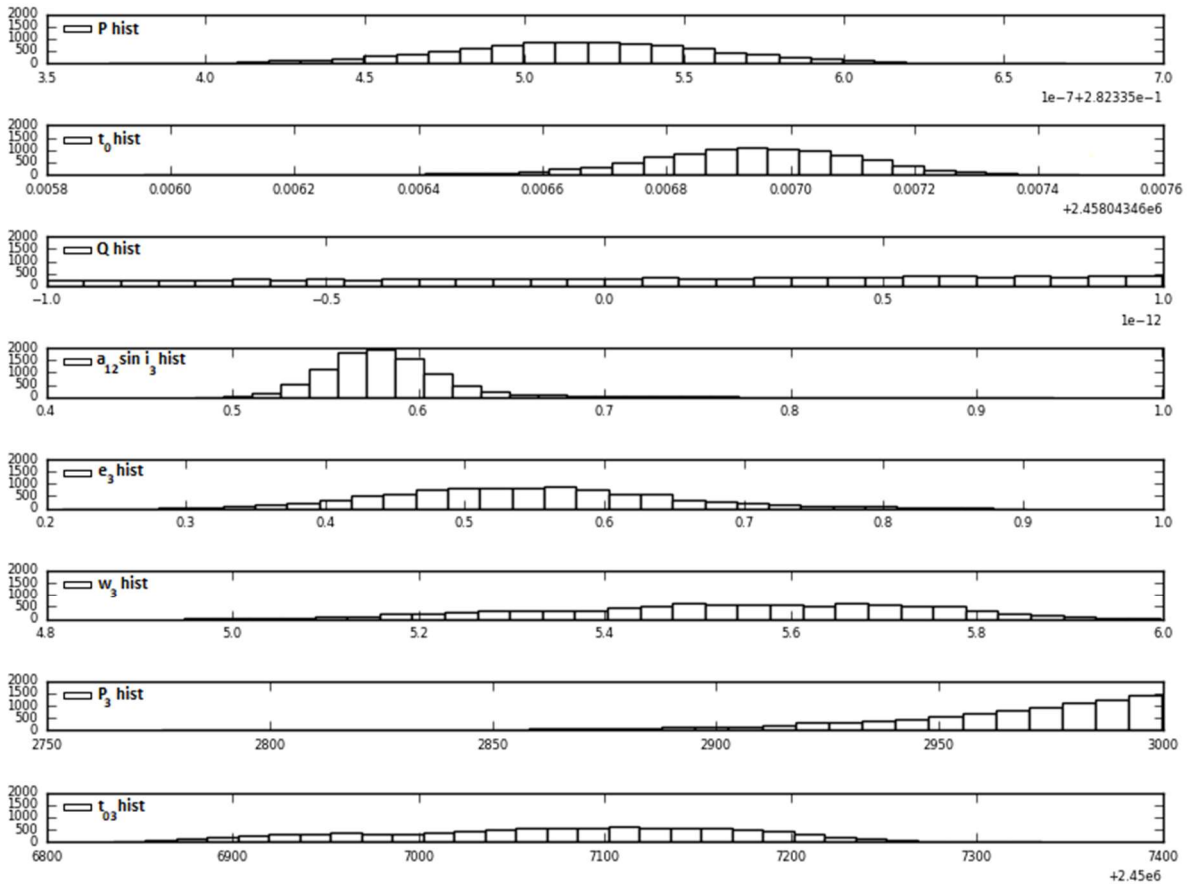


**Fig 10.** Histograms of parameters resulting from the MCMC chain for the LiTE + Quadratic model.

To estimate the quality of the statistical model and to compare models, in addition to  $\chi^2$  and  $\chi^2 = \frac{\chi^2}{n-g}$  statistics in which  $n$  is the number of data points in the fit and  $g$  is the number of fit-parameters, we employed the Bayesian Information Criterion (BIC) defined as:

$$BIC = \chi^2 + k \ln n \quad (10)$$

where  $k$  is the number of variable parameters in the model fit.

**Table 7.** Results from the LITE + Quadratic model for the third body in BQ Ari.

Parameter	Value	Error
$P_3$ [days]	2960.9	34.2
$P_3$ [years]	8.106	0.093
$a_{12} \sin i_3$ [AU]	0.584	0.042
$e_3$	0.54	0.10
$t_{03}$ [BJD <sub>TDB</sub> ]	2457074	98
$\omega_3$ [degree]	317.05	11.34
$K_3$ [minutes]	4.455	0.419
$f(m_3)$ [ $M_\odot$ ]	0.0030	0.0006
$\chi^2$	315.76	
$\chi^2_{red}$	14.35	
BIC	342.97	

Alternatively, the changes in the period could be explained by quadratic + magnetic activity (Applegate 1992). The large-scale orbital period variation of BQ Ari might have also been caused by a magnetic activity cycle and/or spot-induced modulations in the light curves and we assumed this cycle as sinusoidal. The light curve solutions required a huge cold spot due to the differences in the light levels of maxima of the light curves, indicates a significant magnetic activity present in this binary system. This trend reveals a cyclic oscillation with an amplitude of  $A = 5.118$  minutes shown in Figure 11.

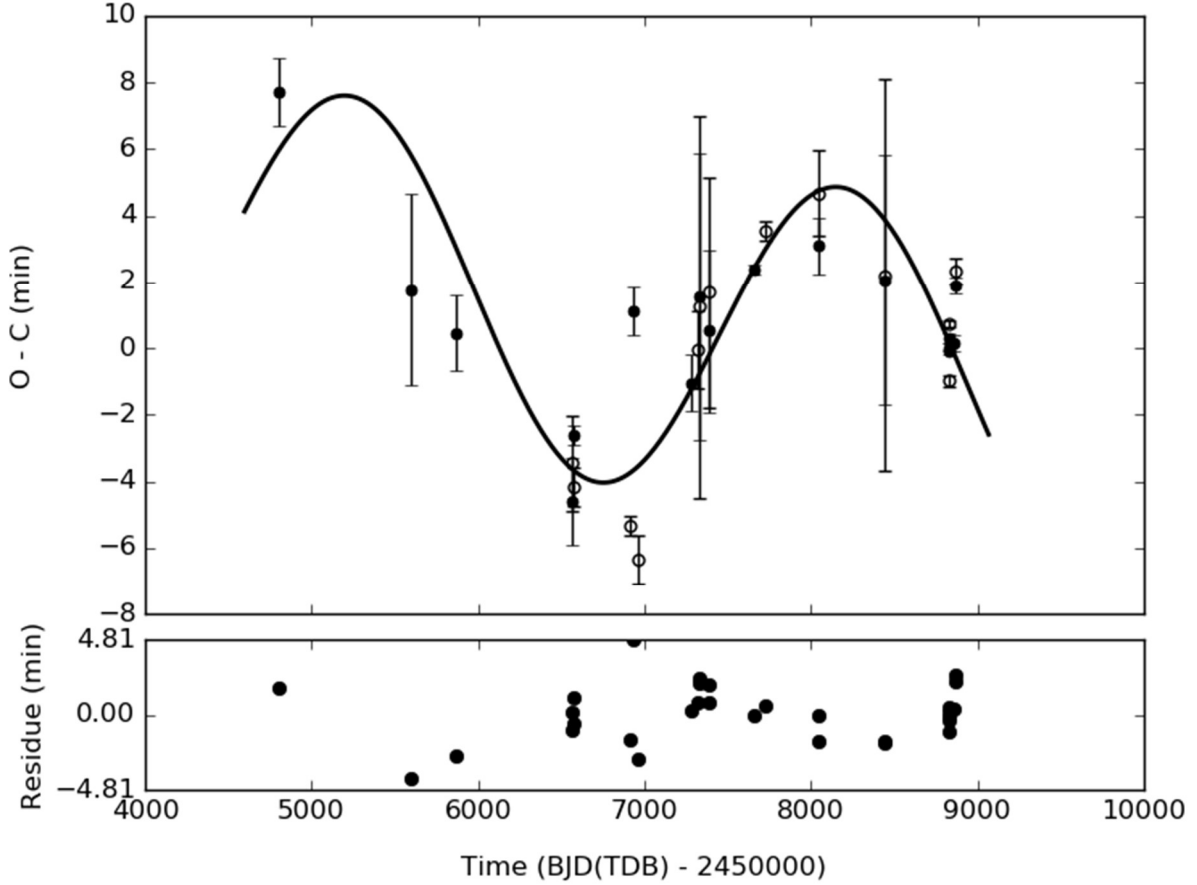


Fig 11. The O-C diagram of BQ Ari with the cyclic trend on the data points induced by the magnetic activity cycle.

The results of the fit applied by the OCFit code are provided in Table 8. The resulting parameters were used to calculate the magnetic circulation model parameters (Applegate 1992). Explanations of the Applegate model application could be found in many eclipsing binary orbital period variation studies (e.g. Soydogan 2008, Mitnyan et al. 2018). As a result of Applegate model, primary component' sub-surface magnetic field strength needs to be 22.6kG for driving that the 8.08 year-long magnetic cycle modulation. Other calculated Applegate parameters are given in Table 9.

Table 8. Results from the magnetic activity model of BQ Ari.

Parameter	Value	Error
$T[days]$	2951.75	35.77
$T[years]$	8.08	0.09
$A[minutes]$	5.118	0.261
$\chi^2$	356.15	
$\chi^2$	16.18	
BIC	383.36	

In two models there is a very small quadratic term in the residue O-C, It reveals a continuous period increase at a rate of  $0.0025 \times 10^{-7} \text{ days/year}$  which corresponds to a period increase of  $0.0022 \text{ s century}^{-1}$ .

**Table 9.** Parameters of applied Applegate model for primary component of BQ Ari.

Parameter	Value
$P_{orb}$ (days)	0.28233566(24)
$A_{mod}$ (days)	0.0036(2)
$P_{mod}$ (days)	2952(36)
$\Delta P$ (s)	0.18
$\Delta P/P$	$7.6 \times 10^{-6}$
$\Delta J$ ( $gcm^2s^{-1}$ )	$1.9 \times 10^{47}$
$I_s$ ( $gcm^2$ )	$5.5 \times 10^{53}$
$\Delta\Omega/\Omega$	0.0013
$\Delta E$ (erg)	$1.3 \times 10^{41}$
$\Delta L_{rms}$ (erg)	$8.3 \times 10^{32}$
$B$ (kG)	22.6
$\Delta m$ (mag)	0.34

## 6 Discussion of the results

We aimed at an investigation of the first light curve and orbital variation analysis of the contact binary system BQ Ari within this study. The photometric observations of BQ Ari were carried out during the four nights of observations using *BVR* filters. We determined its photometric and geometric elements, and their uncertainties with the Wilson-Devinney code based on a Monte Carlo simulation and a mass ratio determined through a  $q$ -search, which gives especially reliable solutions for binary systems with total eclipses. Our results suggest that BQ Ari is a contact binary with a mass ratio of  $0.548 \pm 0.018$  and a fillout factor of 24%, and an inclination of  $85.09 \pm 0.45$ .

In order to study the characteristics of W UMa contact binaries, Xu-Dong Zhang and Sheng-Bang Qian (2020) have collected the data of 370 contact binaries and have plotted the  $P - a$ , and  $M_1 - P$  diagrams. By combining the results of their fits to the data and Kepler's third law, they have presented  $a - P$ , and  $q - P$  relations (Equations 11 and 12), and found a period cut-off for W UMa contact binaries at 0.15 days.

$$a = 10.285 \times P + 0.00155 \quad (11)$$

$$\log_{10}(1 + q) = 3\log_{10}(10.285 \times P + 0.00155) - 2\log_{10}P - \log_{10}(\sqrt{5198 \times P + 2.097} - 1.481) \quad (12)$$

where  $q$  is the mass ratio,  $M_1$  is the mass of more massive component in solar mass unit,  $a$  is separation between two components, and  $P$  is orbital period in year(s). The boundaries of these relations were given as,

$$a_u = 11.587 \times P + 0.00132 \quad (13)$$

$$a_l = 9.972 \times P + 0.00132 \quad (14)$$

$$\log_{10}(1 + q)_u = 3\log_{10}(11.587 \times P + 0.00132) - 2\log_{10}P - \log_{10}(\sqrt{4021 \times P + 1.868} - 1.300) \quad (15)$$

$$\log_{10}(1 + q)_l = 3\log_{10}(9.972 \times P + 0.00132) - 2\log_{10}P - \log_{10}(\sqrt{2701 \times P - 0.967} + 0.104) \quad (16)$$

We have derived  $a$  and  $q$  by using the above equations for BQ Ari and the results are shown in Table 10, which in a very good agreement with the findings of our study.

**Table 10.** The results of using  $a - P$ ,  $q - P$  and boundaries relations to compare for BQ Ari.

Parameter	This Study	Xu-Dong Zhang and Sheng-Bang Qian (2020)		
		Calculated	Lower limit	Upper limit
$a(R_{\odot})$	2.079	2.036	1.935	2.202
$q$	0.548	0.449	0.060	2.482

We suggest a new ephemeris to determine the times of the primary minima for future observations. Since there is a sinusoidal trend in the residuals of the O-C diagram, we provided the alternative solutions; a "LiTE + Quadratic" model and a "Magnetic activity + Quadratic" model. We attempted to explain the residuals of the linear fit in O-C diagram with these two models, and the best models resulted in  $\chi_{red}^2$  values larger than 14.35. LiTE interpretation resulted in an object with a mass function of  $f(m_3) = 0.003 M_{\odot}$  at an average distance of 0.58 AU with highly eccentric orbit  $\sim 0.5$ . This value can be regarded to be too large for an unseen third body, which cannot significantly contribute to the total light of the system, and hence cannot be verified independently.

The O'Connell effect can be recognized clearly in the light curves from our observations (Table 5). We also found a light curve in the B.R.N.O. from the year 2017. This was observed by Školník using the Digital Single-Lens Reflex (DSLR) method with a Clear filter. We calculated the difference between the maxima level of this light curve and found a value of  $MaxI - MaxII = -0.038$ . Although the quality of the light curve is not ideal, the difference between the light levels of the quadrature orbital phases is quite noticeable. On the other hand, light curve solutions required a huge cold spot accounting for the O'Connell effect and the observed light curve asymmetries, which hints at a significant magnetic activity in this binary system. Therefore, fitting the orbital period change with a magnetic activity assumption (cyclic) is also probable, the period of which was calculated to be 8.08 years and  $\Delta P / P = 7.6 \times 10^{-6}$  with expected light changes amplitude,  $\Delta m = 0.34 mag$  from the analysis of the O-C curve. Considering that the magnetic field strength in late spectral type stars generally take values from a few gauss to a few kilo gauss (e.g. Saar 1990, Reiners 2012, Shulyak et al. 2017), it can be said that the magnetic field we found for the primary component (22.6kG) is unusual for this type stars. This strength magnetic field structure can be checked with future spectropolarimetric observations. Also, it is also suggested that there is a longer magnetic cycle perhaps far longer than our observations. It is likely that if we had additional high-quality data, we would be able to reach a better fit with lower  $\chi_{red}^2$  for the "Magnetic activity + Quadratic" model. The system should be followed up to reveal the nature of orbital period variations in it. Hence these models can be considered as speculations for future reference.

There is no radial-velocity information currently available for this binary system, so we were forced to estimate the absolute parameters of the binary system based on a mass ratio found from a  $q$ -search. However, it is well known that the  $q$ -search method works fine for the cases of observed total eclipses (Rucinski 1969), like that for BQ Ari. Based on the method used in this study, we measured a distance of  $128 \pm 19$  pc for the binary system from combined bolometric magnitude derived from our analysis, which is in agreement with the Gaia DR2 value of  $132.848 \pm 1.574$  pc in one standard deviation.

Based on the estimation of the absolute parameters, the components' positions on the H-R diagram are shown in Figure 12. The diagrams of the Mass-Radius (M-R) and Mass-Luminosity (M-L) on a  $\log$ -scale (Figure 13) show the evolutionary status of BQ Ari. Increasing number of such contact binary stars are important for binary stellar evolution model studies and better determination of MLR relations.



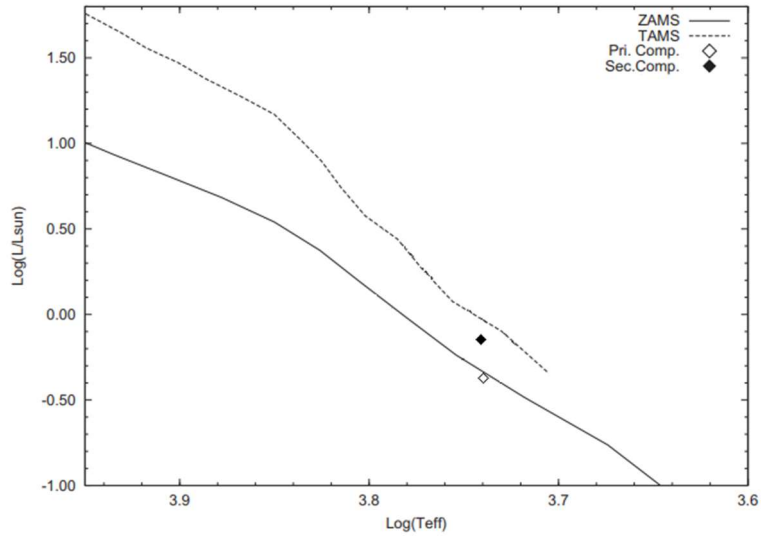


**Fig 12.** Positions of both components of BQ Ari on the H-R diagram. The theoretical ZAMS (solid) and TAMS (dashed) lines are depicted in the diagram.

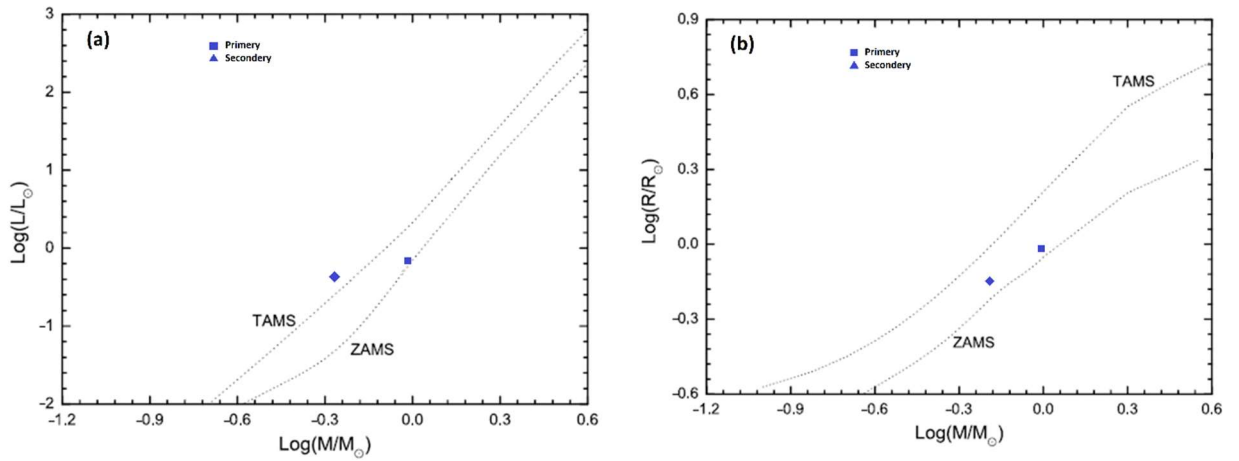


**Fig 13.** The  $\log M - \log R$ , and  $\log M - \log L$  diagrams for BQ Ari from the absolute parameters.

## Acknowledgments

This manuscript was prepared by a joint cooperation between the International Occultation Timing Association Middle East section (IOTA/ME) and Çukurova University of Adana, Adana, Turkey. This group activity occurred during the IOTA/ME 2nd Workshop on Photometric Study of Binary Systems and Exoplanet Transits held at Çukurova University, Adana, Turkey, from 4-7 February 2020.

OB thanks TÜBİTAK for their support with the project 118F042 that made his participation possible. We thank TÜBİTAK National Observatory for its support in providing the CCD to UZAYMER. We also give special thanks to Prof. Mehmet Emin Özel for his cooperation. Furthermore, thanks to Paul D. Maley to make some corrections in the text.

## References

[1] Applegate, J.H., 1992. A mechanism for orbital period modulation in close binaries. *The Astrophysical Journal*, 385, pp.621-629.

[2] Collins, K.A., Kielkopf, J.F., Stassun, K.G. and Hessman, F.V., 2017. AstrolmageJ: image processing and photometric extraction for ultra-precise astronomical light curves. *The Astronomical Journal*, 153(2), p.77. <https://doi.org/10.3847/1538-3881/153/2/77>.

- [3] Csizmadia, S. and Klagyivik, P., 2004. On the properties of contact binary stars. *Astronomy & Astrophysics*, 426(3), pp.1001-1005.
- [4] Davoudi, F., Jafarzadeh, S.J., Poro, A., Basturk, O., Mesforoush, S., Harandi, A.F., Gozarandi, M.J., Mehrjardi, Z.Z., Maley, P.D., Khakpash, S. and Rokni, K., 2020. Light curve analysis of ground-based data from exoplanets transit database. *New Astronomy*, 76, p.101305. <https://doi.org/10.1016/j.newast.2019.101305>.
- [5] Eggen, O.J. and Iben Jr, I., 1989. Starbursts, blue stragglers, and binary stars in local superclusters and groups. II-The old disk and halo populations. *The Astronomical Journal*, 97, pp.431-457.
- [6] Eker, Z., Soydugan, F., Bilir, S., Bakis, V., Alicavus, F., Ozer, S., Aslan, G., Alpsoy, M. and Kose, Y., 2020. Empirical Bolometric Correction Coefficients for Nearby Main-Sequence Stars in Gaia Era. *arXiv preprint arXiv:2006.01836*.
- [7] Fitzpatrick, E.L., 1999. Correcting for the effects of interstellar extinction. *Publications of the Astronomical Society of the Pacific*, 111(755), p.63.
- [8] Gajdoš, P. and Parimucha, S., 2019. New tool with GUI for fitting OC diagrams. *Open European Journal on Variable Stars*, 197, p.71.
- [9] Hübscher, J., 2014., BAV-Results of Observations - Photoelectric Minima of selected Eclipsing Binaries and Maxima of Pulsating Stars., *Information Bulletin on Variable Stars*, 6118.
- [10] Hübscher, J., 2017., BAV-Results of Observations - Photoelectric Minima of selected Eclipsing Binaries and Maxima of Pulsating Stars., *Information Bulletin on Variable Stars*, 6196. DOI: 10.22444/IBVS.6196.
- [11] Hübscher, J. and Lehmann, P.B., 2012. BAV-results of observations-photoelectric minima of selected eclipsing binaries and maxima of pulsating stars. *Information Bulletin on Variable Stars*, 6026.
- [12] Hübscher, J., Lehmann, P.B., Monninger, G., Steinbach, H.M. and Walter, F., 2010. BAV-Results of Observations-Photoelectric Minima of Selected Eclipsing Binaries and Maxima of Pulsating Stars. *IBVS*, 5918, p.1.
- [13] Høg, E., Fabricius, C., Makarov, V.V., Bastian, U., Schwekendiek, P., Wicenec, A., Urban, S., Corbin, T. and Wycoff, G., 2000. Construction and verification of the Tycho-2 Catalogue. *Astronomy and Astrophysics*, 357, pp.367-386.
- [14] Kopal, Z., 1959. *Close Binary Systems*, 1959cbs. book.
- [15] Irwin, J.B., 1952. The Determination of a Light-Time Orbit. *The Astrophysical Journal*, 116, p.211.
- [16] Sriram, K., Malu, S., Choi, C.S. and Rao, P.V., 2017. A Study of the Kepler K2 Variable EPIC 211957146 Exhibiting a Variable O'Connell Effect. *The Astronomical Journal*, 153(5), p.231. <https://doi.org/10.3847/1538-3881/aa6893>.
- [17] Kjurkchieva, D.P., Popov, V.A. and Petrov, N.I., 2019. Global Parameters of 12 Totally Eclipsing W UMa Stars. *The Astronomical Journal*, 158(5), p.186. <https://doi.org/10.3847/1538-3881/ab4203>.
- [18] Kwee, K. and Van Woerden, H., 1956. A method for computing accurately the epoch of minimum of an eclipsing variable. *Bulletin of the Astronomical Institutes of the Netherlands*, 12, p.327.

- [19] Li, M.C.A., Rattenbury, N.J., Bond, I.A., Sumi, T., Bennett, D.P., Koshimoto, N., Abe, F., Asakura, Y., Barry, R., Bhattacharya, A. and Donachie, M., 2018. A study of the light travel time effect in short-period MOA eclipsing binaries via eclipse timing. *Monthly Notices of the Royal Astronomical Society*, 480(4), pp.4557-4577. <https://doi.org/10.1093/mnras/sty2104>.
- [20] Li, X.Z. and Liu, L., 2020. Photometric study of five kepler contact binaries. *New Astronomy*, 81, p.101445. <https://doi.org/10.1016/j.newast.2020.101445>.
- [21] Lucy, L.B., 1967. Gravity-darkening for stars with convective envelopes. *Zeitschrift fur Astrophysik*, 65, p.89.
- [22] Mikulášek, Z., Chrastina, M., Zejda, M., Janík, J., Yhu, L. and Qian, S., 2013. Kwee-van Woerden method: To use or not to use?. arXiv preprint arXiv:1311.0207.
- [23] Mitnyan, T., Bódi, A., Szalai, T., Vinkó, J., Szatmáry, K., Borkovits, T., Bíró, B.I., Hegedüs, T., Vida, K. and Pál, A., 2018. The contact binary VW Cephei revisited: surface activity and period variation. *Astronomy & Astrophysics*, 612, p.A91. <https://doi.org/10.1051/0004-6361/201731402>.
- [24] Nagai, K., 2016., Visual, CCD and DSLR minima of eclipsing binaries during 2015., *VSOLJ Variable Star Bull* (ISSN 0917-2211), 61.
- [25] O'Connell, D.J.K., 1951. The so-called periastron effect in eclipsing binaries. *Monthly Notices of the Royal Astronomical Society*, 111(6), pp.642-642.
- [26] Ozavci, I., Bahar, E., Izci, D.D., Ozuyar, D., Karadeniz, O., SAYAR, B., TORUN, S., ÜZÜMCÜ, M., AZIZOGLU, B., NASOLO, Y. and YILMAZ, M., 2019. A list of minima times of some eclipsing binaries. *OPEN EUROPEAN JOURNAL ON VARIABLE STARS*.
- [27] Pagel, L., 2018., BAV-Results of Observations - Photoelectric Minima of selected Eclipsing Binaries and Maxima of Pulsating Stars., *Information Bulletin on Variable Stars*, 6244. DOI: 10.22444/IBVS.6244.
- [28] Pagel L., 2019. BAV-Results of observations - Photoelectric Minima/Maxima of Selected Eclipsing Binaries and Maxima/Minima of Pulsating Stars. BAV Journal No. 031. [https://www.bav-astro.de/images/Up\\_Journal/BAVJ031\\_R4\\_BAVM249.pdf](https://www.bav-astro.de/images/Up_Journal/BAVJ031_R4_BAVM249.pdf)
- [29] Paschke, A., 2011. A list of minima and maxima timings. *Open European Journal on Variable Stars* (ISSN 1801-5964) 0142.
- [30] Paschke, A., 2017., A List of Minima and Maxima Timings., *Open European Journal on Variable Stars*, 181.
- [31] Pi, Q.F., Zhang, L.Y., Bi, S.L., Han, X.L., Wang, D.M. and Lu, H.P., 2017. Magnetic Activity and Period Variation Studies of the Short-period Eclipsing Binaries. II. V1101 Her, AD Phe, and NSV 455 (J011636. 15-394955.7). *The Astronomical Journal*, 154(6), p.260. <https://doi.org/10.3847/1538-3881/aa9438>.
- [32] Pribulla, T., Vaňko, M., Ammler-von Eiff, M., Andreev, M., Aslantürk, A., Awadalla, N., Baluďansky, D., Bonanno, A., Božić, H., Catanzaro, G. and Ćelik, L., 2012. The Dwarf project: Eclipsing binaries—precise clocks to discover exoplanets. *Astronomische Nachrichten*, 333(8), pp.754-766. <https://doi.org/10.1002/asna.201211722>.

- [33] Qian, S.B., Zhang, J., He, J.J., Zhu, L.Y., Zhao, E.G., Shi, X.D., Zhou, X. and Han, Z.T., 2018. Physical Properties and Evolutionary States of EA-type Eclipsing Binaries Observed by LAMOST. *The Astrophysical Journal Supplement Series*, 235(1), p.5. <https://doi.org/10.3847/1538-4365/aaa601>.
- [34] Saar, S.H., 1990. Magnetic Fields on Solar-Like Stars: The First Decade. In Symposium-International Astronomical Union (Vol. 138, pp. 427-441). Cambridge University Press. <https://doi.org/10.1017/S0074180900044430>.
- [35] Salvatier, J., Wiecki, T.V. and Fonnesbeck, C., 2016. Probabilistic programming in Python using PyMC3. *PeerJ Computer Science*, 2, p.e55.
- [36] Schlegel, D.J., Finkbeiner, D.P. and Davis, M., 1998. Application of SFD Dust Maps to Galaxy Counts and CMB Experiments. arXiv preprint astro-ph/9809230.
- [37] Schlafly, E.F. and Finkbeiner, D.P., 2011. Measuring reddening with Sloan Digital Sky Survey stellar spectra and recalibrating SFD. *The Astrophysical Journal*, 737(2), p.103. <https://doi.org/10.1088/0004-637X/737/2/103>.
- [38] Shapley, H., 1948. *Harvard Obs. Mono.* 7, 249.
- [39] Školník V., 2017. Project-Variable Star and Exoplanet Section of the Czech Astronomical Society (B.R.N.O.). <<http://var2.astro.cz/EN/brno/index.php>>.
- [40] Soyduğan, F., 2008. Possible third body effects in the period changes of four Algol binaries: RY Aqr, SZ Her, RV Lyr and V913 Oph. *Astronomische Nachrichten: Astronomical Notes*, 329(6), pp.587-595. <https://doi.org/10.1002/asna.200710972>.
- [41] Stassun, K.G. and Torres, G., 2018. Evidence for a systematic offset of  $-80 \mu\text{as}$  in the Gaia DR2 Parallaxes. *The Astrophysical Journal*, 862(1), p.61. <https://doi.org/10.3847/1538-4357/aaca6c>.
- [42] Stępień, K., 2006. Evolutionary Status of Late-type Contact Binaries: Case of a  $1.2+1 M_{\odot}$  Binary. *Astrophysics and Space Science*, 304(1-4), pp.81-84.
- [43] Reiners, A., 2012. Observations of cool-star magnetic fields. *Living Reviews in Solar Physics*, 9(1), p.1. <https://doi.org/10.12942/lrsp-2012-1>.
- [44] Reiners, D., Engeln, A., Malo, L., Yadav, R., Morin, J. and Kochukhov, O., 2018. Strong dipole magnetic fields in fast rotating fully convective stars. arXiv preprint arXiv:1801.08571.
- [45] Rucinski, S.M., 1969. The proximity effects in close binary systems. II. The bolometric reflection effect for stars with deep convective envelopes. *Acta Astronomica*, 19, p.245.
- [46] Rucinski, S.M., 1996. Eclipsing Binaries in the OGLE Variable Star Catalog. I. W UMa-type Systems as Distance and Population Tracers in Baade's Window. arXiv preprint astro-ph/9607009.
- [47] Van Hamme, W., 1993. New limb-darkening coefficients for modeling binary star light curves. *The Astronomical Journal*, 106, pp.2096-2117.
- [48] Wilson, R.E. and Devinney, E.J., 1971. Realization of accurate close-binary light curves: application to MR Cygni. *The Astrophysical Journal*, 166, p.605.

[49] Zasche, P., Uhlár, R., Kucakova, H., Svoboda, P., Masek, M., 2014. Collection of minima of eclipsing binaries, Information Bulletin on Variable Stars, 6114, p1-19.

[50] ZASCHE, P., UHLÁŘ, R., SVOBODA, P., KUČÁKOVÁ, H., MAŠEK, M., and JURYŠEK, J., 2017. Collection of minima of eclipsing binaries, part III. Information Bulletin on Variable Stars, vol. 63, No. 6204, p. 1-18. ISSN 0374-0676. doi:10.22444/IBVS.6204.

[51] Zhang, X.D., and Qian, S.B., 2020. Orbital period cut-off of W UMa-type contact binaries. Monthly Notices of the Royal Astronomical Society, 497(3), pp.3493-3503. <https://doi.org/10.1093/mnras/staa2166>.

[52] Zola, S., Gazeas, K., Kreiner, J.M., Ogloza, W., Siwak, M., Koziel-Wierzbowska, D., and Winiarski, M., 2010. Physical parameters of components in close binary systems—VII. Monthly Notices of the Royal Astronomical Society, 408(1), pp.464-474. <https://doi.org/10.1111/j.1365-2966.2010.17129.x>.

[53] Zola, S., Rucinski, S.M., Baran, A., Ogloza, W., Pych, W., Kreiner, J.M., Stachowski, G., Gazeas, K., Niarchos, P. and Siwak, M., 2004. Physical parameters of components in close binary systems: III. Acta Astronomica, 54, pp.299-312.